

Injectable Fluorescent Neural Interfaces for Cell-Specific Stimulating and Imaging

Shumao Xu,[‡] Xiao Xiao,[‡] Farid Manshahi, and Jun Chen*



Cite This: *Nano Lett.* 2024, 24, 4703–4716



Read Online

ACCESS |



Metrics & More



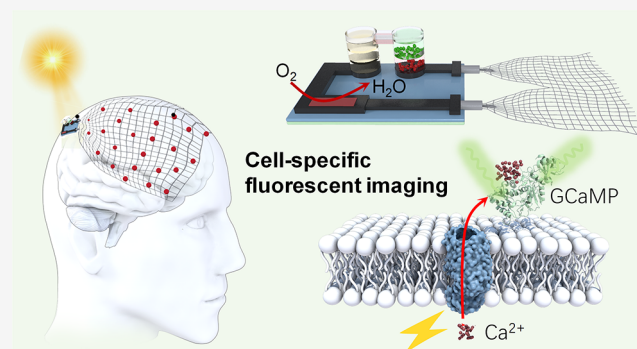
Article Recommendations



Supporting Information

ABSTRACT: Building on current explorations in chronic optical neural interfaces, it is essential to address the risk of photothermal damage in traditional optogenetics. By focusing on calcium fluorescence for imaging rather than stimulation, injectable fluorescent neural interfaces significantly minimize photothermal damage and improve the accuracy of neuronal imaging. Key advancements including the use of injectable microelectronics for targeted electrical stimulation and their integration with cell-specific genetically encoded calcium indicators have been discussed. These injectable electronics that allow for post-treatment retrieval offer a minimally invasive solution, enhancing both usability and reliability. Furthermore, the integration of genetically encoded fluorescent calcium indicators with injectable bioelectronics enables precise neuronal recording and imaging of individual neurons. This shift not only minimizes risks such as photothermal conversion but also boosts safety, specificity, and effectiveness of neural imaging. Embracing these advancements represents a significant leap forward in biomedical engineering and neuroscience, paving the way for advanced brain–machine interfaces.

KEYWORDS: fluorescent neural interfaces, calcium fluorescence imaging, injectable bioelectronics, genetically encoded indicators



Deciphering the complex structure of the brain and understanding its intricate mechanisms of neuronal communication have been pivotal in scientific research. The urgency of this endeavor is highlighted by the widespread occurrence of neurodegenerative disorders such as epilepsy, Parkinson's, and Alzheimer's,^{1–4} which impact millions worldwide.

Emerging from the convergence of multiple disciplines and meeting current needs, a significant advancement in the field of neural interface monitoring and modulation is the development of minimally invasive and retrievable chronic brain implants. These devices offer high-resolution monitoring and modulation of neural activity, marking a significant improvement over traditional methods such as low-resolution, noninvasive electroencephalography (EEG),⁵ invasive intracortical electrocorticography (ECoG),^{6,7} or deep brain stimulation (DBS) electrodes,^{8,9} and time-uncontrolled bioabsorbable brain implants.¹⁰ Notably, these devices can be injected and later removed post-treatment—an essential feature for targeted interventions, allowing for the modulation of neuronal activity over extended periods. This prolonged modulation and the possibility of retrieval post-treatment have the potential to induce neural plasticity in conditions like Parkinson's disease,¹¹ potentially easing symptoms such as tremors and stiffness, and manage aberrant neural activity in epilepsy, reducing the severity and frequency of seizures.¹² It

could enhance synaptic connectivity critical to memory function in Alzheimer's disease,¹³ and in depression and schizophrenia, it regulates neurotransmitter levels and neural circuits to stabilize mood and improve cognitive functions. These personalized interventions significantly improve the efficacy of long-term treatment strategies for each condition. The development of such retrievable implants addresses the risks associated with permanent surgical brain implants, which include tissue damage and inflammation, potentially affecting both device performance and patient health. These potential challenges highlight the urgency and necessity for the development of retrievable electrodes, emphasizing the need to minimize invasiveness and integrate energy-harvesting devices to eliminate dependence on external batteries and additional surgeries.

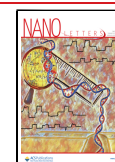
Chronic injectable mesh electronics stand out for their precision in collecting neural signals and the capability to be retrieved after treatment, distinguishing them from conven-

Received: February 15, 2024

Revised: April 5, 2024

Accepted: April 9, 2024

Published: April 12, 2024



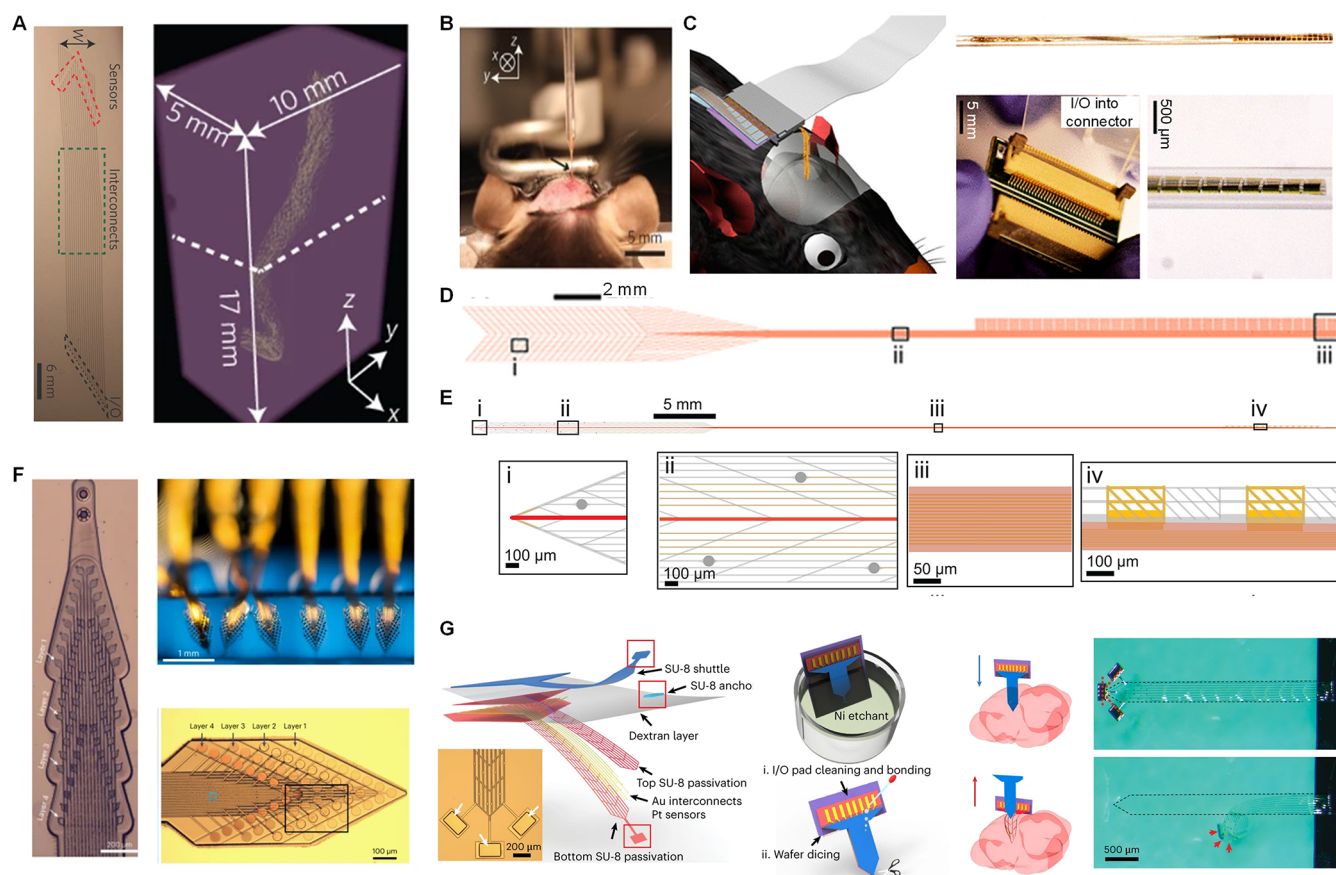


Figure 1. Evolution of injectable electronics and their implantation. (A,B) First-generation injectable mesh electronics. Reproduced with permission from ref 14. Copyright 2015 Springer Nature. (C,D) Second-generation injectable mesh electronics: advancements in I/O interfaces and external connection designs. Reproduced with permission from ref 15. Copyright 2017 American Chemistry Society. (E) Evolved injection-end design of the endovascular probe. Reproduced with permission from ref 16. Copyright 2023 Science. (F) Multilayered, multichannel probes. Reprinted with permission from ref 17. Copyright 2023 Springer Nature. (G) Scalable injectable mesh electronics featuring an injection-end design. Reprinted with permission from ref 18. Copyright 2023 Springer Nature.

tional bulkier Utah arrays and other rigid silicon electrodes. The development of injectable bioelectronics, particularly in flexible, mesh-like structures, has been a significant area of research since 2015. Initially introduced as injectable mesh electronics, it primarily focuses on biocompatibility and appropriate physical properties to ensure safe injection and seamless integration within nervous tissues¹⁴ (Figure 1A,B). By 2017, notable enhancements were made in the input/output interfaces and the design of external connections to improve the reliability of these systems¹⁵ (Figure 1C,D). In 2023, three key advancements were observed in this field: the optimization of the injection-end of endovascular probes¹⁶ (Figure 1E), the development of multilayered and multichannel probes¹⁷ (Figure 1F), and the introduction of scalable injectable mesh electronics¹⁸ (Figure 1G).

■ HARMONIZING FUNCTIONALITY AND PHYSIOLOGY: HOW CAN INJECTABLE MESH ELECTRONICS BRIDGE THE GAP?

Navigating through the intricate field of brain–computer interfaces, considerable progress in neuroscientific imaging has refined methodologies and deepened our understanding of neural activities. The development and refinement of injectable mesh electronics represent a crucial step forward, embodying the integration of technology and biology to achieve a seamless biocompatible interface with brain tissue.^{19,20,19} The fabrica-

tion process typically involves depositing a thermally evaporated nickel sacrificial layer on a silicon wafer, followed by spin-coating with an epoxy-based negative photoresist (SU-8), lithography patterning, deposition of metal interconnects and platinum sensing electrodes, and finally coating with an additional SU-8 passivation layer¹⁴ (Figure 2A,B). Achieving a balance between mechanical durability and biocompatibility with bodily tissues is crucial for the success of chronic neural interfaces. The biocompatibility of mesh electronics within neural environments can be demonstrated through fluorescence imaging (Figure 2C). Polymers like polyimide (PI)^{20–23} and SU-8²⁴ have been identified as preferred materials for substrate and encapsulation, allowing for the design of thicker layers that contribute to the implant's extended durability (Figure 2D). However, this relationship between thickness and durability varies when using materials like polydimethylsiloxane (PDMS)²⁵ and poly(lactic-*co*-glycolic acid) (PLGA)²⁶ for substrate and encapsulation layers, as increased thickness may affect the implant's longevity.

In tackling the inherent challenges of electrode design, size and impedance considerations are crucial for the development of flexible and biocompatible mesh neural electrodes. Reducing the width of conventional metal electrodes to enhance resolution leads to increased impedance, introducing noise and compromising the accuracy of neural recordings^{1,27} (Figure 2E). Thus, a balance between the resolution of the

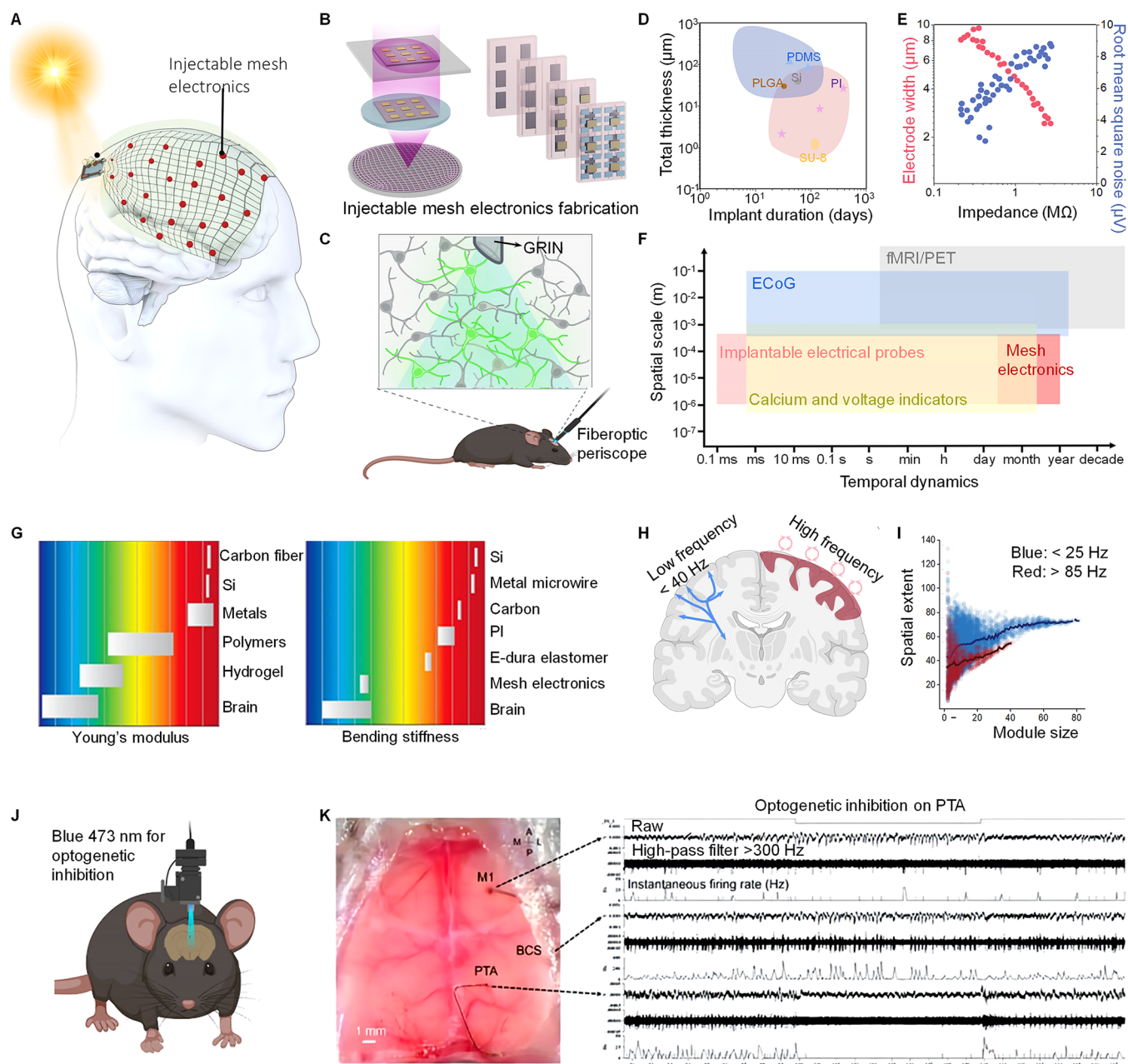


Figure 2. Injectible and retrievable fluorescent neural interfaces. (A) Scheme of the integration of injectable mesh electronics with an external miniaturized solar biofuel cell for self-powered holographic imaging and targeted stimulation. (B) Injectible mesh electronics prepared from lithography. (C) Fiberoptic periscope collecting fluorescence for calcium imaging. (D–G) Electrode integration design. (D) Total thickness versus duration for long-term implantation. Reproduced with permission under a Creative Commons CC-BY 4.0 License from ref 23. Copyright 2020 IOPscience. Red: mechanical robustness determining the implant duration (thicker materials exhibiting a longer duration). Blue: the duration is mainly ascertained by tissue compatibility (thicker materials having a shorter duration). (E) Electrode width and noise versus electrode impedance. Reproduced with permission under a Creative Commons CC-BY 4.0 License from ref 27. Copyright 2015 IEEE. (F) The inclusion of GCaMP in the spatiotemporal dilemma amidst various existing neurotechnologies. Reproduced with permission from ref 1. Copyright 2019 Springer Nature. (G) Young's modulus and bending stiffness of different recording electrodes. Reproduced with permission from ref 1. Copyright 2019 Springer Nature. Blue to red represents an increase in Young's modulus and bending stiffness. (H,I) Frequency modulation for deep tissue stimulation. (H) Evolving insights into ECoG frequency modulation when injecting mesh electronics on brain dura mater surface instead of deep brain tissue. The amplitude of mu/beta rhythm oscillations at low frequency signifies thalamocortical interactions, which can be utilized for stimulating deep brain tissues without causing damage; gamma activity at high frequency denotes local cortical processing; and the ECoG rhythm phase influences this local processing. (I) Spatial extent-module size (number of nodes) relations at different frequencies. Reproduced with permission from ref 36. Copyright 2019 Springer Nature. Low-frequency bands generally exhibit a large spatial extent. (J,K) Blue light stimulation combined with GCaMP for targeted optogenetic inhibition in the posterior thalamic area (PTA). Reproduced with permission under a Creative Commons CC-BY 4.0 License from ref 37. Copyright 2023 eLifesciences. A 473 nm blue light is used to inhibit certain specific proteins, while GCaMP is used for calcium imaging of neuronal activity, revealing how neurons respond to optogenetic modulation.

mesh electrode and the accuracy of the recordings is essential. The incorporation of calcium indicators for real-time observation and modulation of neural activity heralds a new era of augmented spatiotemporal capabilities, improved resolution, and multiplexed functionality in neurotechnology¹ (Figure 2F).

For the longevity and safety of injectable mesh brain implants, it is essential to avoid sharp angles and discontinuities to prevent dense fibrotic reactions and potential severe tissue damage. Designs with small dimensions, like microfibers with diameters below 5.9 μm , can reduce the formation of fibrotic capsules and elicit a mild foreign body response.²⁸ Additionally, overcoming the rigidity of traditional neural electrodes has been a key focus. Materials like carbon fiber and silicon, significantly stiffer than brain tissue, lead to chronic interface alterations and potential damage¹ (Figure 2G). In contrast, SU-8/Pt/SU-8 mesh electronics, with their bending stiffness comparable to that of brain tissue, have traditionally been preferred for addressing these mechanical mismatch issues, preventing tissue scarring, and ensuring imaging longevity.

The field of material science is now moving toward poly(3,4-ethylenedioxythiophene):polystyrenesulfonate (PEDOT:PSS)-based hydrogel electronics as promising alternatives.²⁹ PEDOT:PSS's superior electrical conductivity, over 100 S cm^{-1} in its concentrated dry state and maintaining 15 S cm^{-1} as a hydrogel,³⁰ along with Young's modulus closely matching brain tissue (0.5–10 kPa), underscores its potential as a preferred material for mesh neural electrodes. Recent efforts highlight the viability of 3D printable gel-based devices^{29,30} and their combination with light-curing polymers for lithography fabrication of mesh electronics, emphasizing the importance of maintaining high conductivity and ensuring optical transparency above 90% for effective signal transduction and accurate fluorescence signal capture. To further improve the biocompatibility and extend the functional lifespan, the application of polymer coatings has emerged as a crucial advancement. Polydopamine (PDA), renowned for its biocompatibility and adhesive properties, has been utilized to enhance neural interface integration.^{31,32} Its ability to promote electrode-tissue integration, support neuron growth, and reduce inflammation, when combined with conductive polymers, creates a robust and biocompatible interface that is optimally suited for long-term implantation. Additionally, the use of biomolecules like zwitterionic polymers³³ for antifouling coatings has been instrumental in improving the interface stability, effectively reducing interface degradation, and enhancing the implant's durability. Furthermore, electrochemical copolymerization could be employed to develop coatings for the enhanced durability.³⁴ These polymer coatings, by enhancing the biocompatibility and mechanical harmony of the injectable mesh electronics with the neural tissue, play a pivotal role in realizing the full potential of these neural interfaces for long-term applications.

Exploring injectable mesh electronics' capabilities on the human dura mater surface within ECoG studies reveals their potential to monitor and modulate a spectrum of frequency bands, including mu (8–12 Hz), beta (18–26 Hz), and gamma (above 40 Hz). This detailed application of mesh electronics enriches our understanding of different cognitive processes³⁵ and informs the treatment of neurodegenerative conditions (Figure 2H). The ability to modulate low frequencies below 40 Hz enables deep interactions with neural

networks, while higher frequencies above 40 Hz typically interact with the brain's surface layers, offering diverse insights into neural dynamics. The observed relationship between physical distance and functional connectivity, showing larger modules at lower frequencies³⁶ (Figure 2I), suggests that lower frequency modulation has stronger connections and broader spatial extents than higher frequencies. The recent integration of injectable bioelectronics with genetically encoded calcium indicators (GCaMP) in optogenetics for calcium imaging allows for the monitoring of neuronal activity, enabling researchers to observe neuronal responses to optogenetic modulation³⁷ (Figure 2G,H). These advancements contribute to a more detailed understanding of individual neurons and their neural networks, enhancing our grasp of neuronal dynamics.

■ HOW CAN INJECTABLE MESH ELECTRONICS BE INTEGRATED FOR WIRELESS STIMULATION?

Looking forward, integrating insights from the energy, biological, and technological domains is crucial for the evolution of wireless power and data transmission models. Historically, the dependence on tethered connections for power or data transmission in conventional neural electrodes has restricted the scope and precision of the data collected, impeding natural patient behaviors and, consequently, our grasp of brain functions.³⁸ The advent of wireless brain implants marks the dawn of new possibilities.

Nevertheless, the optimization of wireless brain implant technology faces several hurdles. Current wireless technologies, such as near-field communication (NFC),³⁹ inductive couplings,⁴⁰ ultrasonic communication,⁴¹ Bluetooth,⁴² and other radio frequency (RF) communications,⁴³ often require an additional external device, adding complexity and restricting mobility. A promising direction to overcome the power supply challenge for these implants is the development and integration of miniaturized biofuel and ultrasound energy harvesting devices.^{15,44–46} These cells aim to power injectable neural electrodes independently from external power sources, eliminating the reliance on such sources. This section discusses common energy conversion methods and communication technologies, evaluating the constraints of implantation and the need for auxiliary systems.

Piezoelectricity, known for its relatively high-power conversion rate, is constrained by potential implantation sites, necessitating mechanical stress and movement. The utilization of materials, such as lead zirconate titanate, also raises toxicity concerns, highlighting the importance of cautious implantation considerations. Conversely, electromagnetic conversion, while reducing the need for significant mechanical forces, faces challenges such as mechanical complexity and reduced power outputs. Electrostatic conversion, offering high output power, requires a polarizing circuit to maintain the electric field between variable capacitance plates, adding complexity. Despite triboelectricity's advantages of biocompatibility and straightforward implantation, the need for energy management circuits often results in compromised output power.

Wireless power or transmission technologies typically require external devices. RF communication, utilizing frequencies like 433 MHz, 868 MHz, or 2.4 GHz, can cover several hundred meters, with power consumption from 1 to 100 mW and data rates ranging from 1 Mbps to 2 Gbps.⁴³ However, its susceptibility to interference and the need for additional components, such as antennas and modulators,

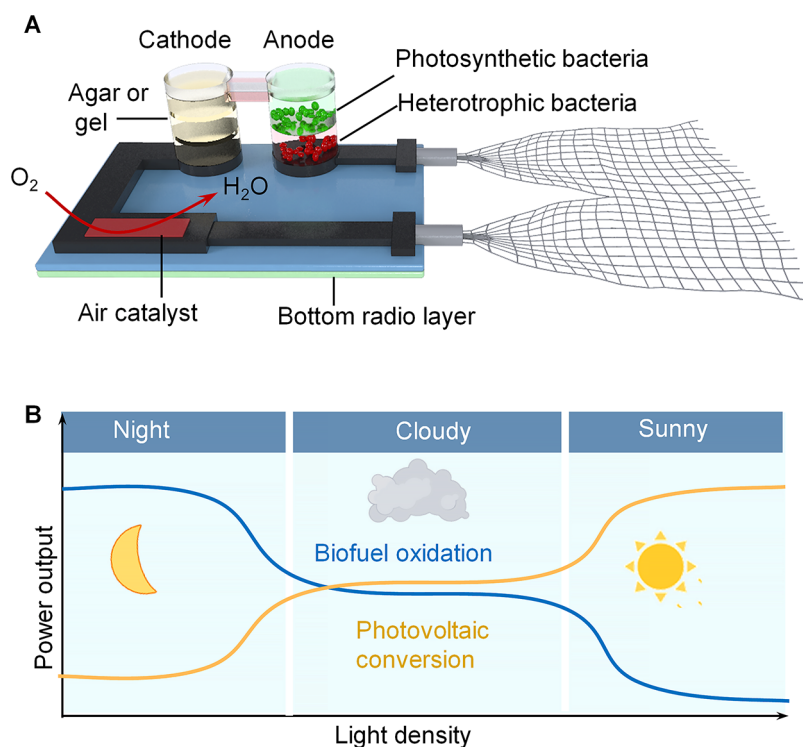


Figure 3. Miniaturized solar biofuel cell for sustainable energy harvesting in brain implants. (A) Schematic of a miniaturized solar biofuel cell system. (B) Dual operational modes of the solar biofuel cell system to ensure a continuous and stable power supply.

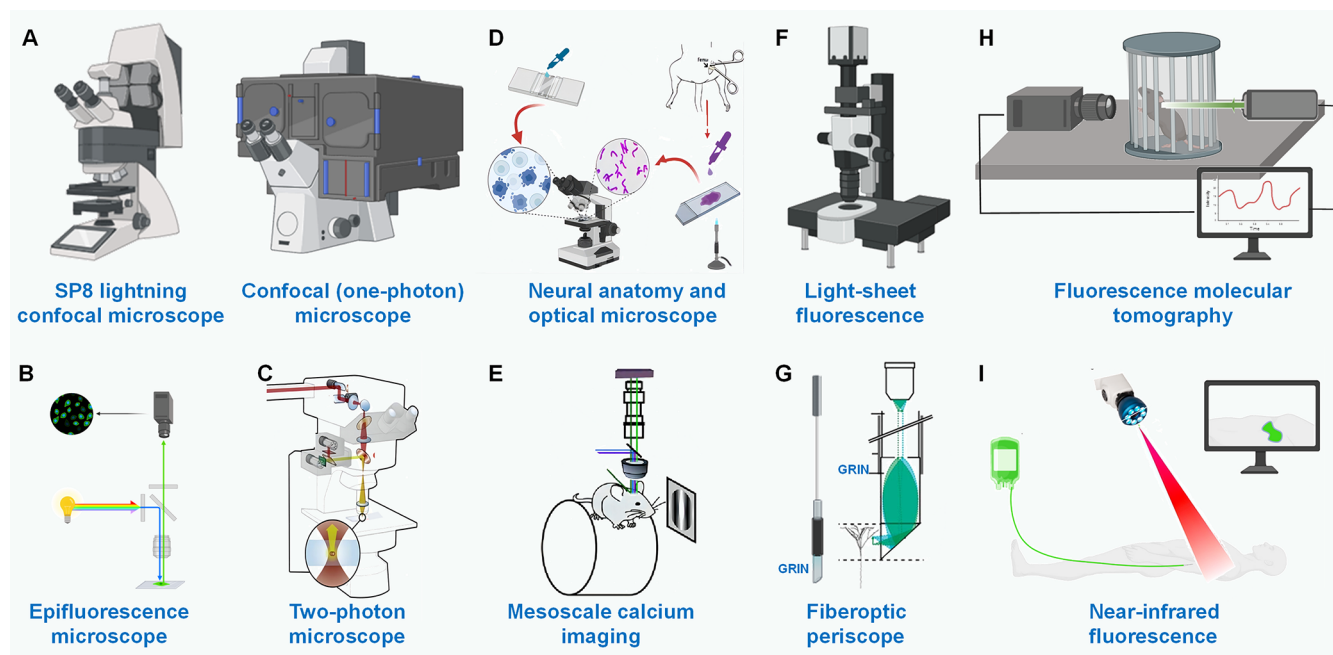


Figure 4. Common fluorescence calcium imaging techniques. (A) Leica TCS SP8 X lightning and typical confocal microscopes; (B) epifluorescence microscope; (C) two-photon microscope; (D) neural anatomy and optical microscope; (E) mesoscale calcium imaging. Reproduced with permission from ref 51. Copyright 2020 Elsevier. (F) Light-sheet fluorescence microscope; (G) fiberoptic periscope. Reproduced with permission from ref 54. Copyright 2009 Springer Nature. (H) Fluorescence molecular tomography; (I) near-infrared fluorescence. Partially created by Biorender.com.

increase the system's complexity. Bluetooth, known for its user-friendliness and operating at microwatt to milliwatt power consumption around 2.4 GHz, is limited by its roughly 100-m range and requires transceivers, posing potential security issues.⁴² NFC operates at 13.56 MHz with a short-range of

typically less than 4 cm, demanding auxiliary devices like a reader (e.g., a smartphone) to initiate communication and a passive chip for data storage and transfer.³⁹ Inductive coupling, efficient but proximity and alignment demanding, typically operates in the low MHz range and requires coils and resonant

Table 1. Comparison of Different Fluorescence Calcium Imaging Techniques

	penetration	resolution	sensitivity ^a	protocol	imaging rates (fpm)	deep tissue imaging	ref.
Epifluorescence microscope	Up to ~200 μm	Submicron	Photon limited	Noninvasive ^b	~60–6000	Limited	47
Confocal (one-photon) microscopy	~100–200 μm	Submicron	Photon limited	Craniotomy	~60–6000	Limited	47
Two-photon microscopy	Up to ~1 mm	Submicron	Photon limited	Craniotomy or window ^c	~60–1800	Limited	48
Mesoscale two-photon imaging	~several hundred μm	Supra-cellular (above micron level)	Photon-limited	Noninvasive ^b	300–600	Limited	50, 51
High-speed 2D light-sheet fluorescence microscopy	NA	Submicron	Photon limited	Craniotomy or window	23,700	Limited	49, 53
Fluorescence molecular tomography	Several cm	1–2 mm	Subnanomolar concentration	Noninvasive	~1	Suitable	57
Near-infrared fluorescence	~1–4 cm	1–3 mm	Submicromolar concentration	Noninvasive	~1	Suitable	58
Fiberoptic periscope with GRIN ^d	Several mm ^e	~2–10 μm	Photon limited	Insertion	~60–6000 ^f	Limited	54, 55

^aPhoton-limited sensitivity highlights the reliance on the photon availability for accurate imaging. Factors such as scattering and absorption can significantly influence the signal quality, influencing the signal-to-noise ratio and the detection capabilities for low-concentration fluorophores.

^bThese noninvasive protocols are often tailored for mice, considering their thinner skulls compared to humans. This anatomical difference allows for easier application of noninvasive imaging techniques. ^cWindow denotes a surgically created opening in the skull for direct access for observation and imaging. ^dGRIN (Gradient Refractive Index): GRIN involves lenses with a varying refractive index, enabling more effective focusing of light through complex tissue structures. ^eThe depth of penetration can vary depending on the length of the probe. ^fThis imaging speed can vary depending on factors including light source intensity, detector sensitivity, resolution, frame averaging, region size, imaging depth, signal-to-noise ratio, and lens properties.

tanks.⁴⁰ Ultrasonic communication, suited for high ambient noise environments, varies in effectiveness and power consumption based on the medium and frequency, utilizing frequencies above 20 kHz and requiring transducers.⁴¹

Harnessing the sun's nearly infinite energy, solar biofuel cells offer a sustainable electricity source. This technology leverages sunlight and the chemical potential of biological materials, such as glucose, to produce a continuous energy flow, thus eliminating the need for external charging.⁴⁴ These cells excel at miniaturization, paving the way for their use in developing compact and efficient brain implants (Figure 3A). A typical single-channel neural electrode requires 10 to 100 μW of power.⁴⁵ However, a miniaturized solar biofuel cell can generate around 500 mV, providing a stable power output of about 5 $\mu\text{W cm}^{-2}$.⁴⁴ For higher power needs, auxiliary solutions such as direct current (DC) to DC booster converters or parallel-connected cells might be used. By daylight, they employ photovoltaic conversion to exploit solar energy, while at night or in low light, they can switch to biofuel oxidation for consistent power (Figure 3B). This versatility ensures a continuous power supply for brain implants. Furthermore, integrating wireless radio layers at the bottom enhances their utility,⁴⁶ enabling real-time energy management and transmission of various biological signals, including neuronal firing patterns and neurotransmitter levels.

■ HOW HAVE FLUORESCENCE IMAGING ADVANCES OVERCOME DEEP BRAIN IMAGING CHALLENGES?

Traditional imaging techniques such as confocal microscopy and epifluorescence microscopy (Figure 4A,B) offer valuable insights into the superficial layers of tissue, achieving depths of up to approximately 200 μm . However, these techniques are limited by the skull's thickness⁴⁷ (Table 1). The Leica SP8 confocal microscopy, with its advanced lightning detection for resolution enhancement, improves imaging capabilities but still faces challenges when penetrating thick biological barriers such as the skull.

In comparison, two-photon microscopy, with its capacity to extend imaging depth to millimeter levels⁴⁸ (Figure 4C), marks a significant advancement in deep brain structure imaging, albeit with limitations in noninvasive applications. Recent development of neural anatomy and optical microscopy (NAOMi) further enhances the evaluation of two-photon microscopies by improving the analysis of large anatomical volumes and facilitating realistic simulations of calcium imaging data sets⁴⁹ (Figure 4D). NAOMi emerges as a promising platform for comparing segmentation algorithms and refining optical designs, driving forward the capabilities of high-resolution imaging. Simultaneously, mesoscale calcium imaging offers a noninvasive approach suitable for nonsurgical GCaMP imaging, capable of capturing large neuronal populations with a penetration depth of several hundred micrometers^{50,51} (Figure 4E), aligning well with the proximity of injectable mesh electronics to neuronal populations. High-speed two-dimensional light-sheet fluorescence microscopy (LSFM) stands out for its ability to capture dynamic cellular events (Figure 4F) at ultrafast rates of up to 23,700 frames per minute (fpm).^{52,53} This efficiency is achieved with a focused light sheet that illuminates the specimen perpendicular to the detection axis, reducing the overall exposure to excitation light. This selective illumination ensures that only the plane of interest within the specimen is exposed to the light sheet, reducing photobleaching and phototoxic effects that are common in conventional wide-field and confocal microscopy. By minimizing light exposure and efficiently separating excitation and emission light paths, LSFM enables high-resolution, three-dimensional imaging of living organisms, including sensitive specimens like developing embryos and brain tissues, and remains compatible with GCaMP for dynamic biological process observation without compromising cell viability. Despite its advantages, LSFM is currently limited by the need for craniotomy to gain optical access, posing a challenge to its broader use in noninvasive calcium imaging. Integrating mesoscale calcium imaging with high-resolution imaging techniques such as NAOMi and LSFM provides a

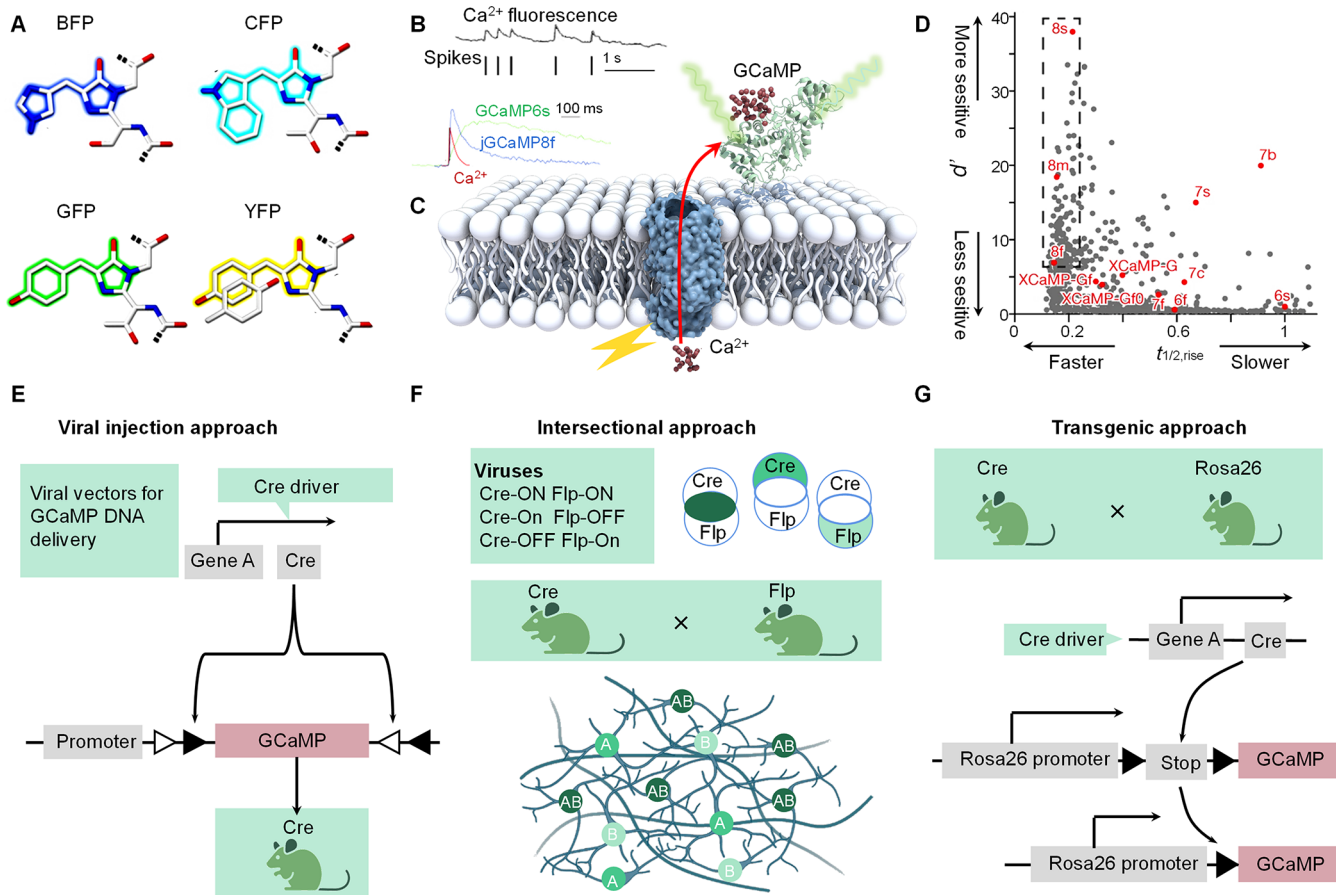


Figure 5. Visualization and analysis of calcium dynamics using GCaMP imaging. (A) Four common chromophores derived from aequorin: blue, cyan, green, and yellow fluorescent proteins (FP). Reproduced with permission from ref 61. Copyright 2007 Biologists. (B) Spikes-induced fluorescence response, and representative fluorescent spectra variations in calcium ions, GCaMP6s, and jGCaMP8f in a cortical pyramidal neuron post-action potential. Reproduced with permission from refs 80, 81. Copyright 2023 Wiley and 2012 Elsevier. The representation highlights different rise and decay time scales, with jGCaMP8f aligning more closely with calcium ions than GCaMP6s. (C) Calcium fluorescent imaging process for neural signal wireless visualization. GCaMP functions as a calcium sensor; when calcium ions enter the cell, they bind to GCaMP, causing it to fluoresce. This fluorescence can then be detected and is indicative of the calcium levels and, consequently, neural activity. (D) Sensitivity, and kinetics analysis of cutting-edge jGCaMP8 variants, normalized to GCaMP6s. Reproduced with permission under a Creative Commons CC-BY 4.0 License from ref 76. Copyright 2023 Springer Nature. (E–G) Potential approaches for expression of GCaMP for cell-specific targeting. (E) Viral injection approach for fluorescence in targeted cell types or regions: modify the virus to contain the GCaMP DNA, inject it into the desired brain region, and use Cre-dependent viral vectors in animals expressing Cre recombinase for precise cell-specific GCaMP expression in calcium imaging. The “Promoter” is a DNA segment that initiates the transcription of GCaMP, effectively regulating its expression in response to specific cellular conditions or stimuli. (F) Intersectional approach for fluorescence in targeted cell subsets uses both Cre-dependent and Flp-dependent viruses to target GCaMP expression within a mixed cell population for studying calcium dynamics in different neuronal subtypes and gaining detailed insights into their activities. Cre and Flp are recombinases that recognize specific DNA sequences (loxP and FRT sites, respectively). When present, they catalyze the recombination of these sequences, leading to targeted gene modifications. Activation of specific genes by Cre or Flp results in the expression of GCaMP, allowing for targeted calcium imaging in specific cell populations. Various viral combinations, such as Cre-ON Flp-ON, Cre-On Flp-OFF, and others, are designed to regulate the expression of genes based on the presence or absence of the Cre and Flp recombinases. For instance, Cre-ON Flp-ON activates gene expression only when both Cre and Flp recombinases are present, while Cre-ON Flp-OFF requires the presence of Cre but the absence of Flp for gene activation. Using these combinations enables precise targeting of specific cell subsets, ensuring GCaMP is expressed exclusively in cells aligned with the criteria determined by the viral combination. (G) Transgenic approach for GCaMP expression in genetically modified organisms creates transgenic mice expressing GCaMP under Cre-dependent control by modifying the Rosa26 mouse and inserting STOP cassettes flanked by recombinase recognition sequences. This enables precise study of various brain and peripheral cell subtypes, avoiding issues like inconsistent spread and transduction efficiency linked to viral vectors.

comprehensive toolkit for analyzing the brain’s functional structure from microscale neuronal interactions to macroscale network dynamics.

The unique structure of mesh electrodes also enables exploration into fiberoptic periscope imaging, which includes targeted loading and horizontal fluorescence collection^{54,55} (Figure 4G). This approach could integrate neural stimulation, fluorescent calcium responses, and images into a comprehensive neural electrode, paving the way for a versatile and

inclusive high-resolution strategy for neural imaging. Advances in fiber photometry and miniaturized microscopes, effectively used in animal models,⁵⁶ allow correlating cellular activity with real-time changes in metabolic parameters or behaviors. Fluorescence molecular tomography (FMT) and near-infrared fluorescence (NIRF) imaging stand out as promising alternatives (Figure 4H,I), with FMT can penetrate from several millimeters to centimeters,⁵⁷ and NIRF achieving penetration depths of up to approximately 4 cm,⁵⁸ allowing for

Table 2. Characteristics of Diverse Ca²⁺ Indicators

indicator type	subtype	K _d (nM) ^a	absorption maxima (nm)	emission maxima (nm)	description
Monomeric (Nonratiometric)	Quin2	115	352/332	492/498	High affinity (low K _d); suitable for detecting low Ca ²⁺ levels Limited targeting and precision Application via injection
	Fluo-2/8c	380	492	514	Moderate affinity, broad use for various cellular activities, nonspecific targeting
	Fluo-3	400	503/506	526	Similar to Fluo-2/8c, potential for cells with higher Ca ²⁺ dynamics
	Fluo-4	345	491/494	~516/516	Enhanced fluorescence and photostability
	Calcium green-1	190	506	531	High sensitivity and increased brightness; ideal for high-resolution imaging
	Calcium green-2	550	506/503	536	For higher Ca ²⁺ levels with moderate affinity
	Calcium green-5 ^N	0.014	506	532	Extremely low K _d , highly sensitive; ideal for very low Ca ²⁺ levels
	Oregon green 488 BAPTA-1	170	494	523	High sensitivity, similar to Calcium green-1; ideal for neurons and muscle cells
	Oregon green 488 BAPTA-2	580	494	523	For high Ca ²⁺ levels, similar to Calcium green-2
	Rhod-2	0.001	556/553	576	Extremely sensitive, ideal for detecting single Ca ²⁺ and targeted imaging with modification
	Calcium orange	328	549	575/576	For a range of Ca ²⁺ levels, with longer wavelength emissions for deeper tissue imaging
	Calcium Crimson	185	589	615	For deeper tissue imaging with near-infrared emission, high sensitivity
	Dextran-conjugated (Nonratiometric) ^b	Fluo-4 dextran (MW 10,000)	~600	~494	~518/518
Calcium green-1 dextran (MW 3000–70,000)		~240–540 ^c	~509	~534	For dynamic range of Ca ²⁺
Oregon green 488 BAPTA-1 dextran (MW 10,000)		~265	~496	~524/524	Improved localization and reduced leakage, ideal for long-term imaging
Monomeric (Ratiometric) ^d	Fura-2	224	362/335	512/505	Wide applications but requiring calibration
	Fura red	140	473/436	670/655	Complementary signal to Fura-2, far-red emission, reducing autofluorescence and light scattering for accurate Ca ²⁺ detection, ideal for multiple indicators
	Indo-1	250	349/331	485/410	UV excitation with dual emission peaks allows for precise ratiometric analysis in Ca ²⁺ changes
Dextran-conjugated (Ratiometric)	Fura-2 dextran (MW 10,000)	~240	364/338	501/494	Combines benefits of Fura-2 with dextran conjugation for targeted, long-term Ca ²⁺ monitoring in specific tissues or cell types
GCaMP variants ^e	GCaMP6s	~200	488	509	Sensitive to neuronal activity, for imaging with moderate Ca ²⁺ levels
	GCaMP6f				Fast kinetics for tracking rapid Ca ²⁺ changes, ideal for detailed neuronal activity studies
	GCaMP6m				Balances sensitivity and temporal resolution for various applications
	jGCaMP7f				Enhanced sensitivity and signal-to-noise ratio for detecting single action potentials and subtle neuronal activities
	GCaMP8 series (GCaMP8f, GCaMP8m)				Enhanced sensitivity, dynamic range, and faster kinetics for neuronal imaging

^aThe dissociation constant (K_d) quantifies the affinity between a ligand and its receptor. A low K_d indicates high affinity, ideal for detecting subtle changes. ^bDextran conjugation limits diffusion, thus improving targeting and reducing cellular toxicity. ^cRange of K_d values originate from dextran sizes, offering versatility in application. ^dDual-wavelength excitation allows for ratiometric measurements, enhancing precise Ca²⁺ quantification. ^eGCaMP offers specific, long-term, and precise monitoring of Ca²⁺ levels in targeted neurons by fluorescing upon Ca²⁺ binding, unlike traditional chemical dyes that lack specificity, have limited duration due to dilution or degradation, and offer lower precision by affecting multiple cell types.

visualization of deep structures at the cost of resolution. When considering nonsurgical calcium imaging for injectable brain implants, selecting the most suitable imaging techniques involves balancing depth, resolution, and imaging protocols. For applications where mesh electronics are placed on the dura mater, depth penetration might be less critical than the resolution and application method, potentially favoring the fiber-optic periscope for its high resolution. However, the optimal choice hinges on the specific needs of each application. In DBS scenarios, where depth penetration is crucial, techniques such as NIRF or FMT might be more appropriate, despite their lower resolution. The integration of advanced

imaging techniques with injectable fluorescent neural interfaces holds promise for real-time, high-resolution monitoring of neuronal activity, offering insights into the interplay between individual neuron functions and physiological responses.

■ HOW DOES GCAMP OUTPERFORM CONVENTIONAL CALCIUM INDICATORS?

The discovery of jellyfish luminescence led to the integration of fluorescence in cellular and molecular imaging,⁵⁹ significantly after the isolation of green fluorescent protein (GFP) by Shimomura in 1962,⁶⁰ marking a significant advancement in biological research. The development of fluorescent proteins,

including yellow, blue, cyan, and red variants, expanded the toolkit for biological studies, particularly in calcium imaging (Figure 5A). Each protein contains a fluorophore—a large polycyclic aromatic hydrocarbon—allowing for the visualization of various cellular components and processes.⁶¹

GCaMP, a fusion protein combining a circularly permuted GFP, calmodulin, and M13 peptide, stands out for its dynamic response to calcium ion binding. This responsiveness surpasses traditional calcium indicators like Fura-2, Indo-1, and Fluo-4, which have dissociation constants (K_d) of 224, 250, and 345 nM, respectively⁶² (Table 2). Traditional calcium indicators rely on chemically synthesized dyes and various loading methods, such as microinjection (typically administered at a concentration of 200 μ M) and acetoxymethyl ester loading, achieving limited penetration depths of approximately 50 μ m.⁶³ In contrast, GCaMP offers significant advantages, including precision in delivery and targeted expression,⁶⁴ achieving spatial resolution down to individual dendritic spines.^{56,65} This precision is crucial in detailed neural activity observation.⁶⁶ Genetic manipulation techniques, like viral vector⁶⁷ and transgenic approaches,^{68,69} enable selective GCaMP expression in specific cell types or compartments, facilitating customization and sustained imaging over months. This specificity allows for the detailed monitoring and decoding of distinct neural networks and individual neuron activities.³⁸ Furthermore, GCaMP's enhanced stability and prolonged imaging duration, enduring continuous illumination for hours,⁷⁰ along with its consistent and reliable signal production, are instrumental for analyzing chronic neural activity changes.⁷¹

In contrast to traditional indicators that suffer from photobleaching and washout, constraining *in vivo* imaging or calcium sensing duration and effectiveness,⁷² various GCaMP versions have been developed. These variants boast a broad dynamic range, with fluorescence changes up to 30-fold, and diverse spectral properties, emitting wavelengths from 500 to 600 nm.⁷³ These features can be tailored for rapid response times in the millisecond range or high sensitivity with nanomolar detection limits, meeting the needs of holographic imaging and targeted stimulation. This adaptability is crucial when integrating with injectable, biocompatible mesh electronics for accurate and real-time neural activity monitoring.

While GCaMP exhibits significant biocompatibility for *in vivo* applications, exploring its potential cellular toxicity is imperative for brain implants. Variants like GCaMP6m and jGCaMP7 can detect subtle changes in single action potentials but may affect neuronal morphology and calcium dynamics differently.⁷⁴ Advances in GCaMP technology include genetic modifications and the introduction of peptides such as RS20, leading to the development of fast and sensitive sensors such as XCaMP and R-CaMP2. Efforts to refine delivery methods have also helped to reduce toxicity. GCaMP-XC, a recent innovation, shows promise with its reduced toxic effects and faster kinetics, offering strategies to balance the toxicity and efficacy of the calcium indicator *in vivo*.⁷⁴ GCaMP's intricate composition, targeted delivery with micron-level resolution, exceptional stability, versatile kinetics, and seamless wireless compatibility make it an optimal choice for imaging^{75,76} when integrated with mesh electrodes in brain implants. This integration holds the potential to enhance the wireless decoding and imaging of large neural populations, addressing challenges often faced with conventional indicators due to their toxicity and limited compatibility.

■ HOW HAVE ADVANCES IN GCaMP DEEPENED OUR UNDERSTANDING OF NEURONAL COMMUNICATION?

Fluorescence plays a vital role in uncovering the complexities of neuronal activity, and calcium, serving as a universal second messenger, is fundamental to cellular signaling across all organisms and acts as a representative indicator of neuronal activity.^{77–79} The relationship between calcium dynamics and neuronal activity has been extensively studied, utilizing various genetically encoded calcium indicators like jGCaMP8f, jGCaMP8m, and jGCaMP6s^{75,76,80,81} (Figure 5B). These indicators are crucial in correlating changes in fluorescence with variations in activity across different sensors and cell populations. The development and application of GCaMP have been pivotal in exploring the intricacies of calcium signaling within neurons, which are essential for neuronal communication and plasticity (Figure 5C). A balance between electrical stimulation and calcium concentration within neurons is maintained by a variety of cellular structures, ion channels, and regulatory proteins, each playing a significant role in modulating neuronal responses.⁸²

Advances such as the temporal oversampling method, which reduces the power requirement and minimizes phototoxic damage,^{83,84} have been crucial in enabling stable *in vivo* recording of single-spine calcium signals. Calcium imaging, therefore, is not confined to mapping global cellular activity but extends to mapping localized dendritic and single-spine calcium responses to sensory stimuli. Genetically encoded calcium indicators, as exemplified by indicators like CerTN-L15, specifically tailored for detecting calcium transients in neurons,⁸⁵ are poised to assume a progressively pivotal role in the examination of dendritic calcium signals. The convergence of refined methodologies—encompassing developments in delivery methods, imaging technology, and signal processing has deepened our understanding of neuronal function and synaptic integration.⁸⁶

The introduction of the jGCaMP8 series has addressed the compromise between resolution and depth penetration inherent in other imaging techniques like FMT and NIRF. Due to its enhanced sensitivity, rapid response, and strong fluorescence,^{76,87} the jGCaMP8 series surpasses its predecessors and rivals, including the XCaMP series (Figure 5D). This breakthrough helps balance the need for high-resolution imaging with the depth penetration required, especially given the challenges of brain tissue properties, and the skull's thickness and opacity. Furthermore, integrating GCaMP indicators with injectable mesh neural electrodes has unlocked new avenues for both fundamental neuroscience research and translational medical applications. This fusion facilitates a deeper exploration and comprehension of the intricate neuronal communications, through which neurons transmit information via electrical and chemical signals to coordinate physiological functions, influence behavior, and support learning and memory within neural networks.⁸⁸ However, it is important to exercise caution with certain GCaMP variants due to their oversensitivity, which can impact the signal-to-noise ratio in densely active neuronal regions.⁸⁹

■ HOW CAN TOOLS AND OPTIMIZATION STRATEGIES FACILITATE THE INTEGRATION OF GCaMP WITH INJECTABLE MESH ELECTRONICS?

Integrating GCaMP indicators with injectable mesh electronics for neuroimaging requires a detailed analysis of the method integration and compatibility. This integration can be achieved through two main approaches. The first approach involves the *in vivo* expression of GCaMP followed by the implantation of neural electrodes. Two primary methods for *in vivo* expression of GCaMP are viral transduction and *in-utero* electroporation. Viral transduction uses viruses as vectors to deliver GCaMP genes into cells, targeting specific brain regions with high precision.^{90–92} This involves engineering a DNA vector within the virus to encode GCaMP (Figure 5E), which is then administered via stereotactic injection. The specificity of GCaMP expression can be enhanced by using a Cre-dependent virus in conjunction with an animal expressing Cre-recombinase. Further refinement is possible through an intersectional approach combining Cre and Flp recombinases (Figure 5F), targeting DNA segments bordered by “loxP” and “FRT” sequences to activate GCaMP expression selectively in specific cell populations. Another approach involves developing transgenic mice that express GCaMP dependent on Cre. This method, utilizing Rosa26 mice, regulates GCaMP expression through one or more STOP cassettes flanked by recombinase recognition sequences⁹³ (Figure 5G). This approach addresses limitations associated with viral vectors such as variable spread and transduction efficiency. *In-utero* electroporation, conversely, introduces DNA plasmids encoding GCaMP into developing embryo precursor cells using electric pulses,⁹⁴ allowing for localized GCaMP expression. Exploration into safe and efficacious delivery is crucial to enhance the long-term stability and biocompatibility of GCaMP. This includes refining viral vectors to improve specificity and diminish immunogenicity. Additionally, understanding the long-term effects of GCaMP expression on neuronal health is essential. This involves evaluating neuronal viability, synaptic functionality, and behavioral outcomes in animal models over time. Through these optimized approaches, the integration of GCaMP with injectable mesh electronics for neuroimaging promises to monitor and understand neural activity with specificity and durability.

The second approach to integrate GCaMP with neural electrodes involves direct attachment methods, leveraging the electrode's surface chemistry. By modifying this surface with chemical groups such as amine, carboxyl, and thiol, a covalent bond with GCaMP can be established.⁹⁵ Bioconjugation techniques also play a role, utilizing specific ligands for binding through interactions such as hydrogen bonding and van der Waals forces. A notable example is the biotin–streptavidin method, where biotinylated GCaMP binds to streptavidin-coated electrodes.⁹⁶ Additionally, electrostatic interactions can be engineered by altering the electrode's charge to attract GCaMP. For example, if GCaMP carries a negative charge at physiological pH (around 7.4), the electrode can be modified with positively charged amine groups for attraction. Conversely, with a positively charged GCaMP, carboxyl groups on the electrode facilitate binding. Optimizing these interactions requires careful control over the surface chemistry and pH levels. Moreover, embedding GCaMP in hydrogels like cross-linked poly(vinyl alcohol) (PVA), polyacrylamide, or alginate provides a stable and compatible interface with neural tissue.

PEDOT:PSS-based gels offer another avenue for integrating GCaMP directly with neural electrodes, ensuring signal stability and tissue compatibility. When choosing integration methods, considerations of efficacy and safety are paramount, with certain methods such as viral injection potentially posing immune response risks.

Incorporating GCaMP into injectable mesh electronics necessitates understanding both the properties of GCaMP and the capabilities of analysis software, such as CIAtah, CaImAn, and SmART2. These tools support calcium imaging with features for motion correction, cell extraction, image analysis, behavior analysis, and data handling.⁸⁵ CIAtah stands out for its versatility in analyzing both one- and two-photon calcium imaging data sets, offering a robust workflow from raw data to insights (Supplementary Table S1). It enhances the clarity and reliability of calcium imaging data through features like movie visualization, preprocessing, multiple cell-extraction methods, and both manual and automated cell classification, ensuring the integrity of recorded neural activity. Additionally, its compatibility with various imaging file formats and adherence to Neurodata standards underline its versatility, marking a significant advancement in calcium imaging analysis.

CaImAn is recognized as an “analysis pipeline” and stands out for its ability to filter out noise, which is crucial in dynamic *in vivo* environments to discern true neuronal signals. This tool is versatile and adaptable, serving as a comprehensive solution across various stages of the calcium imaging analysis. SmART2 specializes in real-time analysis, which is essential for experiments requiring immediate neural feedback or those operating within closed-loop systems. Furthermore, integrating Brainrender into the workflow enhances our understanding of the complex spatial relationships and interactions within neural circuits. Brainrender excels at creating detailed visualizations that map out these networks, providing a 3D view of neural connections, locations of interest, and activity patterns. This software enables visual navigation through the brain's architecture, offering insights into the distribution and dynamics of neural elements such as GCaMP expression, mesh electronics integration, and neuron morphology. The optimization of the hardware specifications is a detailed iterative process involving adjustment, testing, and refinement to achieve the desired performance. This ensures that the mesh electronics are fine-tuned to effectively synchronize with the specific biological environment and GCaMP indicators, resulting in efficient signal transduction, effective light transmission, and accurate capture of fluorescence signals. By strategically aligning the capabilities of the software tools, such as CIAtah, CaImAn, SmART2, and Brainrender, with the optimized specifications of mesh electronics, precise and efficient integration of GCaMP with injectable mesh electronics can be achieved. This ensures that the entire system is poised to provide accurate and reliable insights into neural activity, advancing our understanding of the brain's intricate workings.

The development of injectable and retrievable wireless brain implants represents a notable departure from traditional neural interventions, showcasing a growing demand for nonsurgical yet effective solutions to neural disorders that affect millions globally. These injectable mesh electronics, recognized for their high-resolution monitoring and modulation capabilities, not only facilitate insertion and retrieval post-treatment but also greatly improve long-term therapeutic outcomes and

disease management, emphasizing their significance and potential in clinical applications.

Traditional tethered neural electrodes have limited our exploration of brain mechanisms by restricting patient mobility, thereby hindering in-depth study and intervention. The emergence of wireless technology marks a crucial transition. A major challenge with wireless implants is their reliance on an external apparatus for power or communication. In response, the potential of miniaturized solar biofuel cells has been explored. These cells utilize both sunlight and chemical potential, providing a sustainable and self-sufficient energy source. They adeptly switch between photovoltaic conversion and biofuel oxidation based on lighting conditions, ensuring a constant energy supply. Integrating these cells with wireless radio layers at the bottom boosts their functionality, enabling real-time energy management and continuous neurological monitoring. However, crucial considerations for integrating these miniaturized solar cells include ensuring consistent power generation from biofuel cells to meet the low-power boost converters' input voltage requirements and aligning power output with neural electrode requirements. Beyond leveraging the potential of miniaturized solar biofuel cells for powering brain implants, the integration of GCaMP, a fast and sensitive calcium indicator, is vital in addressing the significant challenges of wireless imaging and stimulating and decoding neural signals.

The translation of GCaMP-based injectable fluorescent neural interfaces for human application encapsulates significant challenges and substantial promise for advancing neurological diagnostics and therapy. Key challenges include the safe delivery and expression of GCaMP within the human brain, overcoming the human skull's imaging barriers, and integrating this technology seamlessly with human physiology. Essential to this endeavor is achieving precise control over GCaMP expression in neurons to ensure accurate and reliable calcium imaging. This requires addressing potential issues, such as alterations in calcium dynamics, the risk of phototoxicity during imaging, artifacts, and variability in expression across cells. Meanwhile, ensuring the safety and biocompatibility of these neural interfaces is essential for minimizing the immune response or dysfunction and maintaining long-term interface stability within the intricate brain environment. Furthermore, the precision in targeting and delivery of neural interfaces, essential for their efficacy, requires advancements in surgical precision, image-guided delivery, and potentially noninvasive methods. Regulatory navigation, encompassing comprehensive trials to further ensure safety and efficacy, alongside addressing ethical concerns related to genetic modifications, represents formidable hurdles yet to be surmounted.

The efficacy of GCaMP determined by their imaging range and depth depends on advancing microscopy techniques. The quest to surmount the challenges of attaining high resolution and deep tissue penetration is a key focus in advancing biomedical imaging. Multiphoton microscopy, leveraging longer wavelength light for deeper penetration with minimal photodamage, benefiting from developments of laser technology and new fluorophores can enhance the depth and resolution of imaging. Further advancements in adaptive optics to correct distortions in the light path promise to significantly improve the resolution of deep tissue imaging. Additionally, tissue-clearing methods, which render tissues transparent to reduce light scattering, are poised for improvements that could facilitate imaging across large volumes of brain tissue.

The fiber-optic periscope emerges as a groundbreaking solution to the challenges of achieving high resolution and penetrating depth in biomedical imaging. By employing a flexible bundle of optical fibers, this periscope offers minimally invasive access to the deep brain structure. Each fiber within the bundle serves as a conduit for light, facilitating high-resolution imaging capabilities at depths that cannot be reached by traditional microscopy. Advancements in fiber optic techniques, including improvements in numerical aperture and light efficiency, promise to further push the boundaries of resolution and depth. When paired with GCaMP fluorescent probes, the fiberoptic periscope stands to reshape real-time monitoring of the intricate dynamics within neural circuits and other cellular entities under direct visualization.

Integrating GCaMP-based fluorescent neural interfaces into adaptive DBS systems enables real-time monitoring of neural activity through electric stimulation-induced GCaMP imaging. This approach allows for immediate adjustments to DBS settings in response to live neural signals, enhancing the precision and effectiveness of treatments while minimizing potential side effects through personalized stimulation.

In summary, injectable and retrievable wireless injectable brain implants, eliminating the need for surgeries, herald a new era in the clinical application of neural modulation, offering precision-targeted treatments for chronic conditions such as Parkinson's disease, epilepsy, and major depressive disorder. The trajectory of injectable wireless fluorescent neural interface is being shaped by strides in energy harvesting devices, the refinement of injectable neural electrodes, and the evolution of calcium imaging techniques. The integration of these technologies into clinical practice could be further supported by continuous improvements in genetic vector designs, delivery mechanisms, and deep brain fluorescent imaging capabilities. These advancements pave the way for a deep understanding of brain functions and the creation of personalized therapeutic strategies, promising clinical brain-implantable treatments for neurological disorders with unprecedented specificity and efficacy.

■ ASSOCIATED CONTENT

Supporting Information

The Supporting Information is available free of charge at <https://pubs.acs.org/doi/10.1021/acs.nanolett.4c00815>.

Supplementary table of Ca²⁺ imaging algorithms and tools (PDF)

■ AUTHOR INFORMATION

Corresponding Author

Jun Chen – Department of Bioengineering, University of California, Los Angeles, Los Angeles, California 90095, United States; orcid.org/0000-0002-3439-0495;
Email: jun.chen@ucla.edu

Authors

Shumao Xu – Department of Bioengineering, University of California, Los Angeles, Los Angeles, California 90095, United States; orcid.org/0000-0003-2062-0226
Xiao Xiao – Department of Bioengineering, University of California, Los Angeles, Los Angeles, California 90095, United States; orcid.org/0000-0002-7861-5596

Farid Manshahi – Department of Bioengineering, University of California, Los Angeles, Los Angeles, California 90095, United States

Complete contact information is available at:
<https://pubs.acs.org/10.1021/acs.nanolett.4c00815>

Author Contributions

[‡]S.X. and X.X. contributed equally to this work.

Notes

The authors declare no competing financial interest.

ACKNOWLEDGMENTS

This is an Invited Review to Prof. Jun Chen by the Editor-in-Chief of *Nano Letters*. The authors acknowledge the Henry Samueli School of Engineering & Applied Science and the Department of Bioengineering at the University of California, Los Angeles for their startup support. J.C. acknowledges the Vernoy Makoto Watanabe Excellence in Research Award at the UCLA Samueli School of Engineering and the Brain & Behavior Research Foundation Young Investigator Grant (Grant Number: 30944). The inception of the wireless brain implant framework highlighted in this work was born at a convergence summit sponsored by the Henry Samueli School of Engineering & Applied Science and the Department of Bioengineering at the University of California, Los Angeles. This transformative vision—injectable, retrievable, and integrated with advanced calcium imaging—was further galvanized by the wireless neural integration project (WNIP). We also extend our acknowledgment to Dr. Julio Alejandro in Prof. Drew's lab and Mr. Hyunjin Lee for the insightful discussions. Further, a nod to the CaImAn, SmAR2, and Brainrender software or tools toward optimizing the calcium imaging modules within our implant framework.

REFERENCES

- (1) Hong, G.; Lieber, C. M. Novel electrode technologies for neural recordings. *Nat. Rev. Neurosci.* **2019**, *20*, 330–345.
- (2) Zhang, H.; Jiang, W.; Zhao, Y.; Song, T.; Xi, Y.; Han, G.; Jin, Y.; Song, M.; Bai, K.; Zhou, J.; Ding, Y. Lipoprotein-inspired nanoscavenger for the three-pronged modulation of microglia-derived neuroinflammation in Alzheimer's disease therapy. *Nano Lett.* **2022**, *22*, 2450–2460.
- (3) Won, S. M.; Cai, L.; Gutruf, P.; Rogers, J. A. Wireless and battery-free technologies for neuroengineering. *Nat. Biomed. Eng.* **2023**, *7*, 405–423.
- (4) Xu, S.; Liu, Y.; Lee, H.; Li, W. Neural interfaces: Bridging the brain to the world beyond healthcare. *Exploration* **2024**, *4*, No. 20230146.
- (5) Drew, L. Decoding the business of brain–computer interfaces. *Nat. Electron.* **2023**, *6*, 90–95.
- (6) Shen, K.; Chen, O.; Edmunds, J. L.; Piech, D. K.; Maharbiz, M. M. Translational opportunities and challenges of invasive electrodes for neural interfaces. *Nat. Biomed. Eng.* **2023**, *7*, 424–442.
- (7) Ramezani, M.; Kim, J.-H.; Liu, X.; Ren, C.; Allothman, A.; De-Eknamkul, C.; Wilson, M. N.; Cubukcu, E.; Gilja, V.; Komiyama, T.; Kuzum, D. High-density transparent graphene arrays for predicting cellular calcium activity at depth from surface potential recordings. *Nat. Nanotechnol.* **2024**, DOI: 10.1038/s41565-023-01576-z.
- (8) Lowet, E.; Kondabolu, K.; Zhou, S.; Mount, R. A.; Wang, Y.; Ravasio, C. R.; Han, X. Deep brain stimulation creates informational lesion through membrane depolarization in mouse hippocampus. *Nat. Commun.* **2022**, *13*, 7709.
- (9) Potel, S. R.; Marceglia, S.; Meoni, S.; Kalia, S. K.; Cury, R. G.; Moro, E. Advances in DBS technology and novel applications: focus on movement disorders. *Curr. Neurol. Neurosci. Rep.* **2022**, *22*, 577–588.
- (10) Zhang, Y.; Lee, G.; Li, S.; Hu, Z.; Zhao, K.; Rogers, J. A. Advances in Bioresorbable Materials and Electronics. *Chem. Rev.* **2023**, *123*, 11722–11773.
- (11) Zhen, K.; Zhang, S.; Tao, X.; Li, G.; Lv, Y.; Yu, L. A systematic review and meta-analysis on effects of aerobic exercise in people with Parkinson's disease. *npj Parkinsons Dis.* **2022**, *8*, 146.
- (12) Knowles, J. K.; Xu, H.; Soane, C.; Batra, A.; Saucedo, T.; Frost, E.; Tam, L. T.; Fraga, D.; Ni, L.; Villar, K.; et al. Maladaptive myelination promotes generalized epilepsy progression. *Nat. Neurosci.* **2022**, *25*, 596–606.
- (13) Liu, C.-C.; Zhao, J.; Fu, Y.; Inoue, Y.; Ren, Y.; Chen, Y.; Doss, S. V.; Shue, F.; Jeevaratnam, S.; Bastea, L.; et al. Peripheral apoE4 enhances Alzheimer's pathology and impairs cognition by compromising cerebrovascular function. *Nat. Neurosci.* **2022**, *25*, 1020–1033.
- (14) Liu, J.; Fu, T.-M.; Cheng, Z.; Hong, G.; Zhou, T.; Jin, L.; Duvvuri, M.; Jiang, Z.; Kruskal, P.; Xie, C.; et al. Syringe-injectable electronics. *Nat. Nanotechnol.* **2015**, *10*, 629–636.
- (15) Schuhmann, T. G., Jr; Yao, J.; Hong, G.; Fu, T.-M.; Lieber, C. M. Syringe-injectable electronics with a plug-and-play input/output interface. *Nano Lett.* **2017**, *17*, 5836–5842.
- (16) Zhang, A.; Mandeville, E. T.; Xu, L.; Sary, C. M.; Lo, E. H.; Lieber, C. M. Ultraflexible endovascular probes for brain recording through micrometer-scale vasculature. *Science* **2023**, *381*, 306–312.
- (17) Le Floch, P.; Zhao, S.; Liu, R.; Molinari, N.; Medina, E.; Shen, H.; Wang, Z.; Kim, J.; Sheng, H.; Partarrieu, S.; et al. 3D spatiotemporally scalable in vivo neural probes based on fluorinated elastomers. *Nat. Nanotechnol.* **2024**, *19*, 319.
- (18) Zhao, S.; Tang, X.; Tian, W.; Partarrieu, S.; Liu, R.; Shen, H.; Lee, J.; Guo, S.; Lin, Z.; Liu, J. Tracking neural activity from the same cells during the entire adult life of mice. *Nature neuroscience* **2023**, *26*, 696–710.
- (19) Li, M.; Li, W.; Guan, Q.; Lv, J.; Wang, Z.; Ding, L.; Li, C.; Saiz, E.; Hou, X. Sweat-resistant bioelectronic skin sensor. *Device* **2023**, *1*, No. 100006.
- (20) Kim, D.-H.; Viventi, J.; Amsden, J. J.; Xiao, J.; Vigeland, L.; Kim, Y.-S.; Blanco, J. A.; Panilaitis, B.; Frechette, E. S.; Contreras, D.; et al. Dissolvable films of silk fibroin for ultrathin conformal bio-integrated electronics. *Nat. Mater.* **2010**, *9*, 511–517.
- (21) Rubehn, B.; Bosman, C.; Oostenveld, R.; Fries, P.; Stieglitz, T. A MEMS-based flexible multichannel ECoG-electrode array. *J. Neural Eng.* **2009**, *6*, No. 036003.
- (22) Chiang, C.-H.; Lee, J.; Wang, C.; Williams, A. J.; Lucas, T. H.; Cohen, Y. E.; Viventi, J. A modular high-density μ ECoG system on macaque vPFC for auditory cognitive decoding. *J. Neural Eng.* **2020**, *17*, No. 046008.
- (23) Araki, T.; Bongartz, L. M.; Kaiju, T.; Takemoto, A.; Tsuruta, S.; Uemura, T.; Sekitani, T. Flexible neural interfaces for brain implants—the pursuit of thinness and high density. *Flex. Print. Electron.* **2020**, *5*, No. 043002.
- (24) Luan, L.; Wei, X.; Zhao, Z.; Siegel, J. J.; Potnis, O.; Tuppen, C. A.; Lin, S.; Kazmi, S.; Fowler, R. A.; Holloway, S.; et al. Ultraflexible nanoelectronic probes form reliable, glial scar-free neural integration. *Sci. Adv.* **2017**, *3*, No. e1601966.
- (25) Tybrandt, K.; Khodagholy, D.; Dielacher, B.; Stauffer, F.; Renz, A. F.; Buzsáki, G.; Vörös, J. High-density stretchable electrode grids for chronic neural recording. *Adv. Mater.* **2018**, *30*, No. 1706520.
- (26) Yu, K. J.; Kuzum, D.; Hwang, S.-W.; Kim, B. H.; Juul, H.; Kim, N. H.; Won, S. M.; Chiang, K.; Trumpis, M.; Richardson, A. G.; et al. Bioresorbable silicon electronics for transient spatiotemporal mapping of electrical activity from the cerebral cortex. *Nat. Mater.* **2016**, *15*, 782–791.
- (27) Scholvin, J.; Kinney, J. P.; Bernstein, J. G.; Moore-Kochlacs, C.; Kopell, N.; Fonstad, C. G.; Boyden, E. S. Close-packed silicon microelectrodes for scalable spatially oversampled neural recording. *IEEE Trans. Biomed. Eng.* **2016**, *63*, 120–130.

- (28) Capuani, S.; Malgir, G.; Chua, C. Y. X.; Grattoni, A. Advanced strategies to thwart foreign body response to implantable devices. *Bioeng. Transl. Med.* **2022**, *7*, No. e10300.
- (29) Yuk, H.; Lu, B.; Lin, S.; Qu, K.; Xu, J.; Luo, J.; Zhao, X. 3D printing of conducting polymers. *Nat. Commun.* **2020**, *11*, 1604.
- (30) Xu, S.; Ahmed, S.; Momin, M.; Hossain, A.; Zhou, T. Unleashing the potential of 3D printing soft materials. *Device* **2023**, *1*, No. 100067.
- (31) Gao, X.; Bao, Y.; Chen, Z.; Lu, J.; Su, T.; Zhang, L.; Ouyang, J. Bioelectronic applications of intrinsically conductive polymers. *Adv. Electron. Mater.* **2023**, *9*, No. 2300082.
- (32) Go, G. T.; Lee, Y.; Seo, D. G.; Lee, T. W. Organic Neuroelectronics: From Neural Interfaces to Neuroprosthetics. *Adv. Mater.* **2022**, *34*, No. 2201864.
- (33) Li, Q.; Wen, C.; Yang, J.; Zhou, X.; Zhu, Y.; Zheng, J.; Cheng, G.; Bai, J.; Xu, T.; Ji, J.; et al. Zwitterionic biomaterials. *Chem. Rev.* **2022**, *122*, 17073–17154.
- (34) Kosuri, S.; Borca, C. H.; Mugnier, H.; Tamasi, M.; Patel, R. A.; Perez, I.; Kumar, S.; Finkel, Z.; Schloss, R.; Cai, L.; et al. Machine-assisted discovery of Chondroitinase ABC complexes toward sustained neural regeneration. *Adv. Healthc. Mater.* **2022**, *11*, No. 2102101.
- (35) Schalk, G.; Leuthardt, E. C. Brain-computer interfaces using electrocorticographic signals. *IEEE Rev. Biomed. Eng.* **2011**, *4*, 140–154.
- (36) Betzel, R. F.; Medaglia, J. D.; Kahn, A. E.; Soffer, J.; Schonhaut, D. R.; Bassett, D. S. Structural, geometric and genetic factors predict interregional brain connectivity patterns probed by electrocorticography. *Nat. Biomed. Eng.* **2019**, *3*, 902–916.
- (37) Xiao, D.; Yan, Y.; Murphy, T. H. Mesotrode allows chronic simultaneous mesoscale cortical imaging and subcortical or peripheral nerve spiking activity recording in mice. *Elife* **2023**, *12*, No. RP87691.
- (38) Xu, S.; Momin, M.; Ahmed, S.; Hossain, A.; Veeramuthu, L.; Pandiyan, A.; Kuo, C. C.; Zhou, T. Illuminating the Brain: Advances and Perspectives in Optoelectronics for Neural Activity Monitoring and Modulation. *Adv. Mater.* **2023**, *35*, No. 2303267.
- (39) Shin, G.; Gomez, A. M.; Al-Hasani, R.; Jeong, Y. R.; Kim, J.; Xie, Z.; Banks, A.; Lee, S. M.; Han, S. Y.; Yoo, C. J.; et al. Flexible near-field wireless optoelectronics as subdermal implants for broad applications in optogenetics. *Neuron* **2017**, *93*, 509–521.
- (40) Manoufali, M.; Bialkowski, K.; Mohammed, B.; Abbosh, A. Wireless power link based on inductive coupling for brain implantable medical devices. *IEEE Antennas Wirel. Propag. Lett.* **2018**, *17*, 160–163.
- (41) Kashani, Z.; Ilham, S. J.; Kiani, M. Design and optimization of ultrasonic links with phased arrays for wireless power transmission to biomedical implants. *IEEE Trans. Biomed. Circuits Syst.* **2022**, *16*, 64–78.
- (42) Kim, C. Y.; Ku, M. J.; Qazi, R.; Nam, H. J.; Park, J. W.; Nam, K. S.; Oh, S.; Kang, I.; Jang, J.-H.; Kim, W. Y.; et al. Soft subdermal implant capable of wireless battery charging and programmable controls for applications in optogenetics. *Nat. Commun.* **2021**, *12*, 535.
- (43) Noormohammadi, R.; Khaleghi, A.; Balasingham, I. Galvanic impulse wireless communication for biomedical implants. *IEEE Access* **2021**, *9*, 38602–38610.
- (44) Mohammadifar, M.; Tahernia, M.; Choi, S. A miniaturized, self-sustaining, and integrable bio-solar power system. *Nano Energy* **2020**, *72*, No. 104668.
- (45) Ng, K. A.; Xu, Y. P. A low-power, high CMRR neural amplifier system employing CMOS inverter-based OTAs with CMFB through supply rails. *IEEE J. Solid State Circuits* **2016**, *51*, 724–737.
- (46) Lee, Y.; Bang, S.; Lee, I.; Kim, Y.; Kim, G.; Ghaed, M. H.; Pannuto, P.; Dutta, P.; Sylvester, D.; Blaauw, D. A modular 1 mm³ die-stacked sensing platform with low power I²C inter-die communication and multi-modal energy harvesting. *IEEE J. Solid State Circuits* **2013**, *48*, 229–243.
- (47) Saini, A.; Kiskey, L. Fluorescence microscopy of biophysical protein dynamics in nanoporous hydrogels. *J. Appl. Phys.* **2019**, *126*, 081101.
- (48) Katona, G.; Szalay, G.; Maák, P.; Kaszás, A.; Veress, M.; Hillier, D.; Chiovini, B.; Vizi, E. S.; Roska, B.; Rózsa, B. Fast two-photon in vivo imaging with three-dimensional random-access scanning in large tissue volumes. *Nat. Methods* **2012**, *9*, 201–208.
- (49) Zhang, Y.; Zhang, G.; Han, X.; Wu, J.; Li, Z.; Li, X.; Xiao, G.; Xie, H.; Fang, L.; Dai, Q. Rapid detection of neurons in widefield calcium imaging datasets after training with synthetic data. *Nat. Methods* **2023**, *20*, 747–754.
- (50) Guillamón-Vivancos, T.; Vandael, D.; Torres, D.; López-Bendito, G.; Martini, F. J. Mesoscale calcium imaging in vivo: evolution and contribution to developmental neuroscience. *Front. Neurosci.* **2023**, *17*, No. 1210199.
- (51) Cardin, J. A.; Crair, M. C.; Higley, M. J. Mesoscopic imaging: shining a wide light on large-scale neural dynamics. *Neuron* **2020**, *108*, 33–43.
- (52) Dvinskikh, L.; Sparks, H.; MacLeod, K. T.; Dunsby, C. High-speed 2D light-sheet fluorescence microscopy enables quantification of spatially varying calcium dynamics in ventricular cardiomyocytes. *Front. Phys.* **2023**, *14*, No. 1079727.
- (53) Stelzer, E. H.; Strobl, F.; Chang, B.-J.; Preusser, F.; Preibisch, S.; McDole, K.; Fiolka, R. Light sheet fluorescence microscopy. *Nat. Rev. Methods Primers* **2021**, *1*, 73.
- (54) Murayama, M.; Larkum, M. E. In vivo dendritic calcium imaging with a fiberoptic periscope system. *Nat. Protoc.* **2009**, *4*, 1551–1559.
- (55) Zhou, B.; Fan, K.; Guo, J.; Feng, J.; Yang, C.; Li, Y.; Shi, S.; Kong, L. Plug-and-play fiber-optic sensors based on engineered cells for neurochemical monitoring at high specificity in freely moving animals. *Sci. Adv.* **2023**, *9*, No. eadg0218.
- (56) Streich, L.; Boffi, J. C.; Wang, L.; Alhalaseh, K.; Barbieri, M.; Rehm, R.; Deivasigamani, S.; Gross, C. T.; Agarwal, A.; Prevedel, R. High-resolution structural and functional deep brain imaging using adaptive optics three-photon microscopy. *Nat. Methods* **2021**, *18*, 1253–1258.
- (57) Ntziachristos, V.; Ripoll, J.; Wang, L. V.; Weissleder, R. Looking and listening to light: the evolution of whole-body photonic imaging. *Nat. Biotechnol.* **2005**, *23*, 313–320.
- (58) Neijenhuis, L. K.; de Myunck, L. D.; Bijlstra, O. D.; Kuppen, P. J.; Hilling, D. E.; Borm, F. J.; Cohen, D.; Mieog, J. S. D.; Steup, W. H.; Braun, J.; et al. Near-infrared fluorescence tumor-targeted imaging in lung cancer: a systematic review. *Life* **2022**, *12*, 446.
- (59) Jia, H.-R.; Zhu, Y.-X.; Duan, Q.-Y.; Wu, F.-G. Cell surface-localized imaging and sensing. *Chem. Soc. Rev.* **2021**, *50*, 6240–6277.
- (60) Shimomura, O.; Johnson, F. H.; Saiga, Y. Extraction, purification and properties of aequorin, a bioluminescent protein from the luminous hydromedusa, *Aequorea*. *J. Comp. Physiol.* **1962**, *59*, 223–239.
- (61) Shaner, N. C.; Patterson, G. H.; Davidson, M. W. Advances in fluorescent protein technology. *J. Cell Sci.* **2007**, *120*, 4247–4260.
- (62) Kao, J. P.; Li, G.; Auston, D. A. Practical aspects of measuring intracellular calcium signals with fluorescent indicators. In *Methods in Cell Biology*; Elsevier: 2010; Vol. 99, pp 113–152.
- (63) Carter, K. P.; Young, A. M.; Palmer, A. E. Fluorescent sensors for measuring metal ions in living systems. *Chem. Rev.* **2014**, *114*, 4564–4601.
- (64) Shemesh, O. A.; Linghu, C.; Piatkevich, K. D.; Goodwin, D.; Celiker, O. T.; Gritton, H. J.; Romano, M. F.; Gao, R.; Yu, C.-C. J.; Tseng, H.-A.; et al. Precision calcium imaging of dense neural populations via a cell-body-targeted calcium indicator. *Neuron* **2020**, *107*, 470–486.
- (65) Kubitschke, M.; Müller, M.; Wallhorn, L.; Pulin, M.; Mittag, M.; Pollok, S.; Ziebarth, T.; Bremshey, S.; Gerdey, J.; Claussen, K. C.; et al. Next generation genetically encoded fluorescent sensors for serotonin. *Nat. Commun.* **2022**, *13*, 7525.

- (66) Machado, T. A.; Kauvar, I. V.; Deisseroth, K. Multiregion neuronal activity: the forest and the trees. *Nat. Rev. Neurosci.* **2022**, *23*, 683–704.
- (67) Kamiya, A.; Hayama, Y.; Kato, S.; Shimomura, A.; Shimomura, T.; Irie, K.; Kaneko, R.; Yanagawa, Y.; Kobayashi, K.; Ochiya, T. Genetic manipulation of autonomic nerve fiber innervation and activity and its effect on breast cancer progression. *Nat. Neurosci.* **2019**, *22*, 1289–1305.
- (68) Bounds, H. A.; Sadahiro, M.; Hendricks, W. D.; Gajowa, M.; Gopakumar, K.; Quintana, D.; Tasic, B.; Daigle, T. L.; Zeng, H.; Oldenburg, I. A.; Adesnik, H. All-optical recreation of naturalistic neural activity with a multifunctional transgenic reporter mouse. *Cell Rep.* **2023**, *42*, 112909.
- (69) Nectow, A. R.; Nestler, E. J. Viral tools for neuroscience. *Nat. Rev. Neurosci.* **2020**, *21*, 669–681.
- (70) Bansal, A.; Shikha, S.; Zhang, Y. Towards translational optogenetics. *Nat. Biomed. Eng.* **2023**, *7*, 349–369.
- (71) Russell, L. E.; Dagleish, H. W.; Nutbrown, R.; Gauld, O. M.; Herrmann, D.; Fişek, M.; Packer, A. M.; Häusser, M. All-optical interrogation of neural circuits in behaving mice. *Nat. Protoc.* **2022**, *17*, 1579–1620.
- (72) Wang, W.; Kim, C. K.; Ting, A. Y. Molecular tools for imaging and recording neuronal activity. *Nat. Chem. Biol.* **2019**, *15*, 101–110.
- (73) Klima, J. C.; Doyle, L. A.; Lee, J. D.; Rappleye, M.; Gagnon, L. A.; Lee, M. Y.; Barros, E. P.; Vorobieva, A. A.; Dou, J.; Bremner, S.; et al. Incorporation of sensing modalities into de novo designed fluorescence-activating proteins. *Nat. Commun.* **2021**, *12*, 856.
- (74) Geng, J.; Tang, Y.; Yu, Z.; Gao, Y.; Li, W.; Lu, Y.; Wang, B.; Zhou, H.; Li, P.; Liu, N. Chronic Ca²⁺ imaging of cortical neurons with long-term expression of GCaMP-X. *Elife* **2022**, *11*, No. e76691, DOI: 10.7554/eLife.76691.
- (75) Dynes, J. L.; Yeromin, A. V.; Cahalan, M. D. Photoswitching alters fluorescence readout of jGCaMP8 Ca²⁺ indicators tethered to Orai1 channels. *Proc. Natl. Acad. Sci. U.S.A.* **2023**, *120*, No. e2309328120.
- (76) Zhang, Y.; Rózsa, M.; Liang, Y.; Bushey, D.; Wei, Z.; Zheng, J.; Reep, D.; Broussard, G. J.; Tsang, A.; Tsegaye, G.; et al. Fast and sensitive GCaMP calcium indicators for imaging neural populations. *Nature* **2023**, *615*, 884–891.
- (77) Emiliani, V.; Entcheva, E.; Hedrich, R.; Hegemann, P.; Konrad, K. R.; Luscher, C.; Mahn, M.; Pan, Z.-H.; Sims, R. R.; Vierock, J.; Yizhar, O. Optogenetics for light control of biological systems. *Nat. Rev. Methods Primers* **2022**, *2*, 55.
- (78) Ippolito, D.; Glauser, D. A. Multiple antagonist calcium-dependent mechanisms control CaM kinase-1 subcellular localization in a *C. elegans* thermal nociceptor. *Elife* **2023**, *12*, No. e85260.
- (79) Hanc, P.; Gonzalez, R. J.; Mazo, I. B.; Wang, Y.; Lambert, T.; Ortiz, G.; Miller, E. W.; von Andrian, U. H. Multimodal control of dendritic cell functions by nociceptors. *Science* **2023**, *379*, No. eabm5658.
- (80) Grienberger, C.; Konnerth, A. Imaging calcium in neurons. *Neuron* **2012**, *73*, 862–885.
- (81) Zhang, Y.; Looger, L. L. Fast and sensitive GCaMP calcium indicators for neuronal imaging. *J. Physiol.* **2023**, DOI: 10.1113/JP283832.
- (82) Zhao, D.; Huang, R.; Gan, J.-M.; Shen, Q.-D. Photoactive Nanomaterials for Wireless Neural Biomimetics, Stimulation, and Regeneration. *ACS Nano* **2022**, *16*, 19892–19912.
- (83) Chen, X.; Leischner, U.; Varga, Z.; Jia, H.; Deca, D.; Rochefort, N. L.; Konnerth, A. LOTOS-based two-photon calcium imaging of dendritic spines in vivo. *Nat. Protoc.* **2012**, *7*, 1818–1829.
- (84) Chen, X.; Leischner, U.; Rochefort, N. L.; Nelken, I.; Konnerth, A. Functional mapping of single spines in cortical neurons in vivo. *Nature* **2011**, *475*, 501–505.
- (85) Mank, M.; Griesbeck, O. Genetically encoded calcium indicators. *Chem. Rev.* **2008**, *108*, 1550–1564.
- (86) Yap, E.-L.; Greenberg, M. E. Activity-regulated transcription: bridging the gap between neural activity and behavior. *Neuron* **2018**, *100*, 330–348.
- (87) Li, J.; Shang, Z.; Chen, J.-H.; Gu, W.; Yao, L.; Yang, X.; Sun, X.; Wang, L.; Wang, T.; Liu, S.; et al. Engineering of NEMO as calcium indicators with large dynamics and high sensitivity. *Nat. Methods* **2023**, *20*, 918–924.
- (88) Mei, J.; Muller, E.; Ramaswamy, S. Informing deep neural networks by multiscale principles of neuromodulatory systems. *Trend Neurosci.* **2022**, *45*, 237–250.
- (89) Tian, L.; Hires, S. A.; Mao, T.; Huber, D.; Chiappe, M. E.; Chalasani, S. H.; Petreanu, L.; Akerboom, J.; McKinney, S. A.; Schreiter, E. R.; et al. Imaging neural activity in worms, flies and mice with improved GCaMP calcium indicators. *Nat. Methods* **2009**, *6*, 875–881.
- (90) Gadella, T. W., Jr; van Weeren, L.; Stouthamer, J.; Hink, M. A.; Wolters, A. H.; Giepmans, B. N.; Aumonier, S.; Dupuy, J.; Royant, A. mScarlet3: a brilliant and fast-maturing red fluorescent protein. *Nat. Methods* **2023**, *20*, 541–545.
- (91) Bindels, D. S.; Postma, M.; Haarbosch, L.; van Weeren, L.; Gadella, T. W., Jr Multiparameter screening method for developing optimized red-fluorescent proteins. *Nat. Protoc.* **2020**, *15*, 450–478.
- (92) Zhang, S.; Ai, H.-w. A general strategy to red-shift green fluorescent protein-based biosensors. *Nat. Chem. Biol.* **2020**, *16*, 1434–1439.
- (93) Mirabella, P. N.; Fenselau, H. Advanced neurobiological tools to interrogate metabolism. *Nat. Rev. Endocrinol.* **2023**, *19*, 639–654.
- (94) dal Maschio, M.; Ghezzi, D.; Bony, G.; Alabastri, A.; Deidda, G.; Brondi, M.; Sato, S. S.; Zaccaria, R. P.; Di Fabrizio, E.; Ratto, G. M.; Cancedda, L. High-performance and site-directed in utero electroporation by a triple-electrode probe. *Nat. Commun.* **2012**, *3*, 960.
- (95) Oh, E. J.; Park, K.; Kim, K. S.; Kim, J.; Yang, J.-A.; Kong, J.-H.; Lee, M. Y.; Hoffman, A. S.; Hahn, S. K. Target specific and long-acting delivery of protein, peptide, and nucleotide therapeutics using hyaluronic acid derivatives. *J. Controlled Release* **2010**, *141*, 2–12.
- (96) Farka, Z.; Mickert, M. J.; Pastucha, M.; Mikušová, Z.; Skládal, P.; Gorris, H. H. Advances in Optical Single-Molecule Detection: En Route to Supersensitive Bioaffinity Assays. *Angew. Chem., Int. Ed.* **2020**, *59*, 10746–10773.